

# The tubular phase of self-avoiding anisotropic crystalline membranes

Mark Bowick\* and Alex Travesset†

Physics Department, Syracuse University,  
Syracuse, NY 13244-1130, USA

## Abstract

We analyze the tubular phase of self-avoiding anisotropic crystalline membranes. A careful analysis using renormalization group arguments together with symmetry requirements motivates the simplest form of the large-distance free energy describing fluctuations of tubular configurations. The non-self-avoiding limit of the model is shown to be exactly solvable. For the full self-avoiding model we compute the critical exponents using an  $\varepsilon$ -expansion about the upper critical embedding dimension for general internal dimension  $D$  and embedding dimension  $d$ . We then exhibit various methods for reliably extrapolating to the physical point ( $D = 2, d = 3$ ). Our most accurate estimates are  $\nu = 0.62$  for the Flory exponent and  $\zeta = 0.80$  for the roughness exponent.

---

\*bowick@physics.syr.edu

†alex@suhep.phy.syr.edu

# 1 Introduction

The statistical mechanics of isotropic crystalline membranes has been the subject of much work in the last ten years [1, 2]. In the absence of *self-avoidance* there is a finite temperature *crumpling* transition from a low-temperature flat (orientationally-ordered) phase to a high-temperature crumpled phase. The novel flat phase of phantom crystalline membranes is by now quite well understood, both qualitatively and quantitatively. The effect of self-avoidance on the phase diagram presents a much greater analytical and numerical challenge. While there is still some controversy, the bulk of evidence at present indicates that the crumpled phase disappears. It is possible, however, that this is the result of bending rigidity induced by next-to-nearest-neighbor excluded volume interactions.

Rather surprisingly, it has been shown [3] that anisotropy has a remarkable effect on the global phase diagram of this class of membranes. For phantom membranes the flat and crumpled phases are isomorphic to those of the isotropic system (anisotropy is irrelevant in these phases) but there are intermediate tubular phases in which the membrane is ordered in one extended direction ( $y$ ) and crumpled in the remaining transverse directions ( $\perp$ ). Since self-avoidance is less constraining for configurations that are crumpled in one direction only, it is very likely that the tubular phase will survive in the more physical self-avoiding case, in contrast to the situation for isotropic membranes. Besides their intrinsic novelty, the study of membranes of this class may have important experimental and practical applications. First of all polymerized membranes with in-plane tilt order would have intrinsic anisotropy. In addition, polymerization in the presence of an applied electric field should produce anisotropic membranes [4].

The key critical exponents characterizing the tubular phase are the size (or Flory) exponent  $\nu$ , giving the scaling of the tubular diameter  $R_g$  with the extended  $L_y$  and transverse  $L_\perp$  sizes of the membrane, and the roughness exponent  $\zeta$  associated with the growth of height fluctuations  $h_{rms}$  (see Fig. 1):

$$\begin{aligned} R_g(L_\perp, L_y) &\propto L_\perp^\nu S_R(L_y/L_\perp^z) \\ h_{rms}(L_\perp, L_y) &\propto L_y^\zeta S_h(L_y/L_\perp^z) \end{aligned} \tag{1}$$

Here  $S_R$  and  $S_h$  are scaling functions [3, 5] and  $z = \frac{\nu}{\zeta}$  is the anisotropy exponent. In the phantom tubular phase (PTP)  $\nu$  and  $\zeta$  were computed in

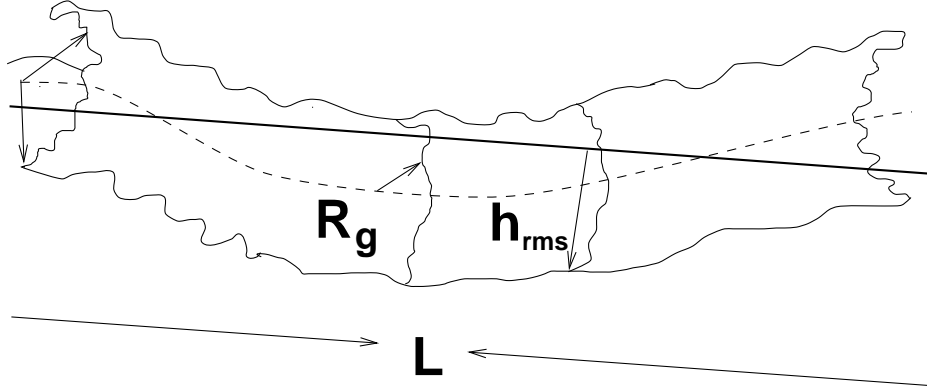


Figure 1: A schematic illustration of a tubular configuration indicating the radius of gyration  $R_g$  and the height fluctuations  $h_{rms}$ .

[3], together with a self-consistent determination of the anomalous elasticity. The existence of the tubular phase has also been confirmed by numerical simulations [7] and the critical exponents measured are in excellent agreement with the theoretical predictions. In this paper we show that a careful analysis of the relevant operators in the free energy allows an *a priori* exact calculation of the anomalous elasticity as well as the above critical exponents.

For self-avoiding membranes the model is much more difficult to treat analytically. By adapting the Edwards model for self-avoiding membranes to the geometry of the tubular phase, Radzihovsky and Toner [3] obtained a model free energy to describe this system. This was further studied by Bowick and Gitter [6], who utilized the multi-local-operator-product-expansion (MOPE)[11, 12] to perform an  $\varepsilon \equiv (d_c^{SA} - d)$  expansion about the upper critical (embedding) dimension  $d_c^{SA} = 11$ . The phase diagram implied by this analysis is shown in Fig. 2. Note the infrared stable fixed point (SAFP) with non-vanishing self-avoidance coupling  $b$  associated with the tubular phase. Bowick and Gitter also showed that the bending rigidity is not renormalized and computed the critical exponents to first order in  $\varepsilon$ . They noted, however, that the extrapolation of these predictions to the physical tubule was not very robust against higher-order perturbations.

Radzihovsky and Toner [5] have argued that the phase diagram described above is actually more complicated (see Fig. 3) for embedding dimension  $d$  less than a critical value  $d_*$ , with  $d_* > 3$ . They argue that the physics below

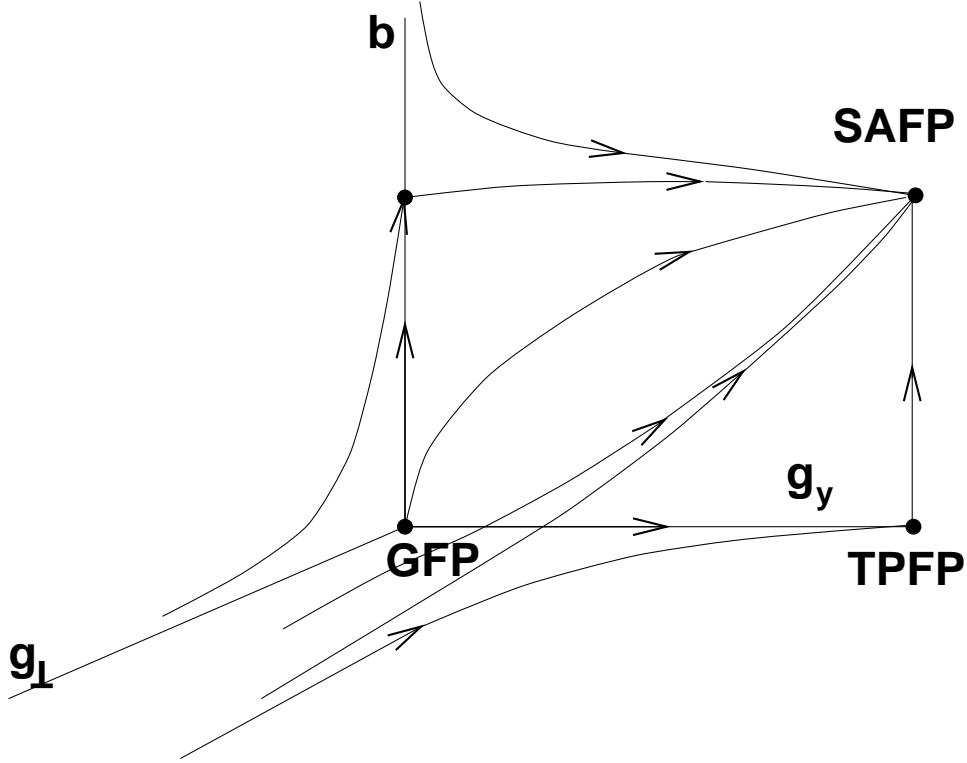


Figure 2: The phase diagram for self-avoiding anisotropic membranes with the Gaussian fixed point (GFP), the tubular phase fixed point (TPFP) and the self-avoidance fixed point (SAFP).

$d^*$  is controlled by a new fixed point (BRFP) which is non-perturbative in  $\varepsilon$ . This postulated fixed point is quite distinct physically from the SAF. In particular the bending rigidity picks up a non-zero anomalous exponent. Calculating critical exponents at the putative BRFP would present the formidable challenge of a complete treatment of both self-avoidance and full non-linear elasticity. Reasonable estimates of  $\nu$  may, however, be obtained within the Flory approximation.

In the present paper we begin with a careful analysis of the rotational symmetries of the tubular problem and their realization within a Wilsonian renormalization group approach [8]. This constrains the possible operators that may appear in the free energy and allows us to identify some operators

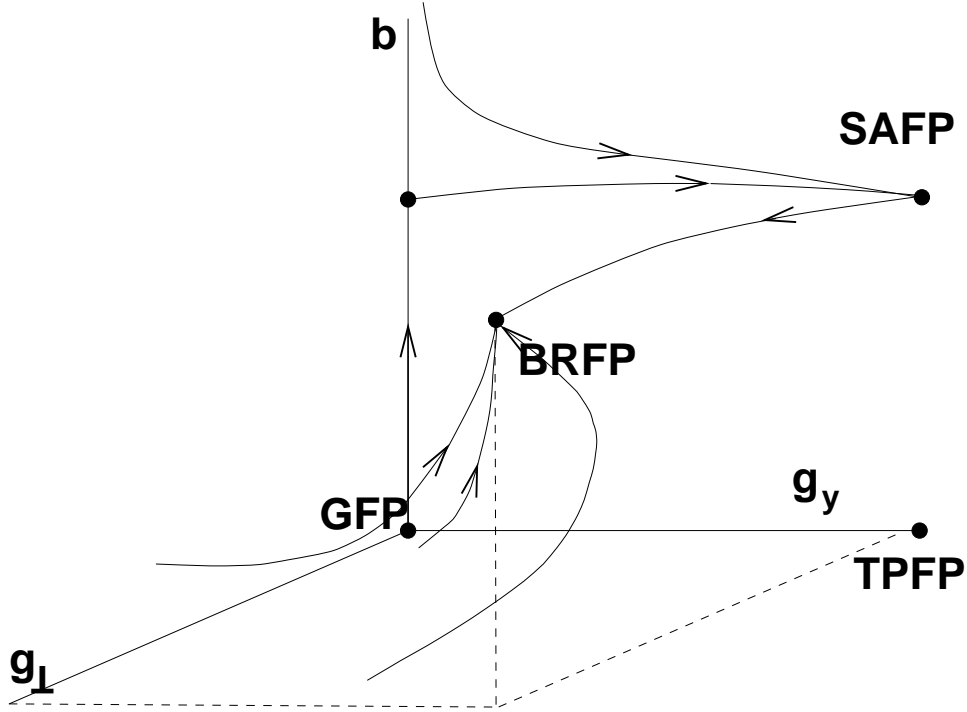


Figure 3: The phase diagram for self-avoiding anisotropic membranes with the Gaussian fixed point (GFP), the tubular phase fixed point (TPFP), the self-avoidance fixed point (SAFP) and the bending rigidity fixed point (BRFP).

as definitely being irrelevant with respect to a broad category of fixed points. As a result of our analysis we can motivate the phase diagram Fig. 2, which follows from the free energy studied in [6], with the incorporation of a relevant operator involving in-plane phonon excitations. The analysis of [5] assumes that non-linear elasticity terms are always irrelevant. It may therefore break down if new terms in the free energy alter the renormalization group flows. While this may change the character of the fixed point above, our analysis suggests that it is imperative to understand the SAFP in as much detail as possible. This is the focus of the present paper. Given the model we next turn to the actual calculation of reliable critical exponents in the tubular phase. This is done by generalizing the calculation of [6] to manifolds of arbitrary internal dimension  $D$  embedded in general dimension  $d$ . We analyze a class

of generalized  $\varepsilon$ -expansions that allow us to determine an optimal path from the line  $\varepsilon = 0$  to the physical point ( $D = 2, d = 3$ ). Our most accurate estimates are

$$\begin{aligned}\nu &= 0.62 \\ \zeta &= 0.80 .\end{aligned}\tag{2}$$

Furthermore, we show that the critical exponents determined in this method are extremely close to the Flory prediction, particularly for  $d > 3$ . This may be regarded as strengthening the predictions of the otherwise uncontrolled Flory approximation.

The outline of our paper is as follows. The model is described in Sec. 2 along with an analysis of its symmetries and their implementation in a Wilsonian renormalization group framework. This leads to a clarification of the global phase diagram and a proposal for the simplest free energy capturing the essential large distance physics of the tubular phase. This is followed in Sec. 3 by a derivation of the scaling relations connecting the fundamental critical exponents. The special case of the phantom tubule is treated in detail in Sec. 4. The full physical problem of the self-avoiding tubule is tackled in Sec. 5, where critical exponents are computed via a generalized  $\varepsilon$ -expansion. We also compute corrections to the Flory and Gaussian variational approximations. A brief summary of our results is given in Sec. 6. Finally, some technical details of the  $\varepsilon$ -expansion are left to the Appendix Sec. A.

## 2 Model

A membrane configuration may be characterized by giving the position  $\vec{r}(\mathbf{x})$ , in the  $d$ -dimensional embedding space, of a point in the membrane labeled by a  $D$ -dimensional internal coordinate  $\mathbf{x}$ . A physical membrane corresponds to the case  $d = 3$  and  $D = 2$ .

In [3, 5] the most general Landau-Ginzburg-Wilson free energy  $F$  for this system is constructed by expanding  $F$  to leading order in powers of  $\vec{r}(\mathbf{x})$  and its gradients with respect to internal space  $\mathbf{x}$ , taking into account global translation and rotational invariance. We will consider the case in which the membrane is isotropic in  $D - 1$  membrane directions (denoted  $\mathbf{x}_\perp$ ) orthogonal

to a distinguished direction  $y$ . The resultant free energy is given by

$$\begin{aligned}
F(\vec{r}(\mathbf{x})) &= \frac{1}{2} \int d^{D-1} \mathbf{x}_\perp dy \left[ \kappa_\perp (\partial_\perp^2 \vec{r})^2 + \kappa_y (\partial_y^2 \vec{r})^2 \right. \\
&\quad + \kappa_{\perp y} \partial_y^2 \vec{r} \cdot \partial_\perp^2 \vec{r} + t_\perp (\partial_\alpha^\perp \vec{r})^2 + t_y (\partial_y \vec{r})^2 \\
&\quad + \frac{u_{\perp\perp}}{2} (\partial_\alpha^\perp \vec{r} \cdot \partial_\beta^\perp \vec{r})^2 + \frac{u_{yy}}{2} (\partial_y \vec{r} \cdot \partial_y \vec{r})^2 \\
&\quad + u_{\perp y} (\partial_\alpha^\perp \vec{r} \cdot \partial_y \vec{r})^2 + \frac{v_{\perp\perp}}{2} (\partial_\alpha^\perp \vec{r} \cdot \partial_\alpha^\perp \vec{r})^2 \\
&\quad \left. + v_{\perp y} (\partial_\alpha^\perp \vec{r})^2 (\partial_y \vec{r})^2 \right] \\
&\quad + \frac{b}{2} \int d^D \mathbf{x} \int d^D \mathbf{x}' \delta^d(\vec{r}(\mathbf{x}) - \vec{r}(\mathbf{x}')), \tag{3}
\end{aligned}$$

where the parameters denote bending and elastic moduli. Note the complexity of this model – it has eleven free parameters. In mean field theory the non-self-avoiding limit ( $b=0$ ) yields a phase diagram with flat and crumpled phases separated by a tubular phase [3].

In this paper we will be mainly concerned with the tubular phase (TP) beyond mean field theory. In this case we may expand  $\vec{r}$  in the Monge representation:

$$\vec{r}(\mathbf{x}) = (\zeta_y y + u(\mathbf{x}), \vec{h}(\mathbf{x})). \tag{4}$$

The free energy is now a function of  $u$  and  $\vec{h}$ . Before simplifying Eq. 3 let us discuss the symmetries of the tubular phase.

Since the free energy must be invariant under global rotations of the tubule it is expressible in terms of the complete set of tubular rotationally invariant operators. These are

$$\begin{aligned}
E(u, h) &= \partial_y u + \frac{1}{2} (\partial_y \vec{h})^2 + \frac{1}{2} (\partial_y u)^2 \\
F_\alpha(u, h) &= \partial_\alpha u + \partial_y \vec{h} \partial_\alpha \vec{h} + \partial_y u \partial_\alpha u \\
F_{\alpha\beta}(u, h) &= \partial_\alpha u \partial_\beta u + \partial_\alpha \vec{h} \partial_\beta \vec{h} \\
G_y(u, h) &= (\partial_y^2 u)^2 + (\partial_y^2 \vec{h})^2 \\
G_{y\alpha\beta}(u, h) &= (\partial_y^2 u) (\partial_{\alpha\beta} u) + \partial_y^2 \vec{h} \partial_{\alpha\beta} \vec{h}. \tag{5}
\end{aligned}$$

Indeed, Eq. 3 becomes

$$F(u, \vec{h}) = \frac{1}{2} \int d^{D-1} \mathbf{x}_\perp dy \left[ 2\zeta_y (t_y + u_{yy} \zeta_y^2) E(u, h) + \kappa_y \zeta_y^4 G_y(u, h) \right]$$

$$\begin{aligned}
& +\kappa_{y\perp}G_{y\alpha}^\alpha(u, h) + 2u_{yy}\zeta_y^4E^2(u, h) + (t_\perp + v_{\perp y})\zeta_y^2F_\alpha^\alpha + \zeta_y^4u_{\perp y}F_\alpha F^\alpha \\
& + 2v_{\perp y}\zeta_y^2E(u, h)F_\alpha^\alpha + \frac{u_{\perp\perp}}{2}F_\beta^\alpha F_\alpha^\beta + \frac{v_{\perp\perp}}{2}(F_\alpha^\alpha)^2 \Big] \\
& + \frac{b}{2} \int d^{D-1}\mathbf{x}_\perp dy d^{D-1}\mathbf{x}'_\perp dy' \delta^{d-1}(\vec{h}(\mathbf{x}_\perp, y) - \vec{h}(\mathbf{x}'_\perp, y')) \\
& \times \delta(\zeta_y(y - y') + u(\mathbf{x}_\perp, y) - u(\mathbf{x}'_\perp, y'))
\end{aligned} \tag{6}$$

Since we are interested in the critical properties of the free energy Eq. 6 we may simplify by dropping irrelevant terms. Simple power counting around the Gaussian fixed point is usually enough to determine the relevancy of operators but in this case the situation is more involved and requires a careful analysis of the symmetries of the problem, to which we turn now.

## 2.1 Wilson RG in the tubular phase

We apply the Renormalization Group (RG) a la Wilson [8] to the free energy Eq. 6. While this approach is usually more involved for extracting actual numbers than the more conventional field theory approach [10], it is more general and allows an easier analysis of the irrelevant operators, key to deciding which terms to retain in the free energy. The crucial point in Wilson RG is the RG transformation. This is a two step procedure: the *blocking* and the *rescaling*.

There is considerable freedom in the choice of blocking. We chose decimation in momentum space, where in order to simplify the calculations an anisotropic spherical momentum regularization is assumed. The blocking just consists in integrating over an anisotropic shell of thickness  $e^{-l}$ ,  $l \in [0, +\infty)$ . That is,

$$e^{-F_l(u, \vec{h})} = \int \prod_{\{|q_\perp|, |q_y|\} \in \mathcal{B}} du(q_\perp, q_y) d\vec{h}(q_\perp, q_y) e^{-F(u, h)}. \tag{7}$$

The region  $\mathcal{B}$  consists of three sectors

$$\mathcal{B} = \begin{cases} 1 > |q_\perp| > e^{-l}, & e^{-zl} > |q_y| > 0 \\ 1 > |q_\perp| > e^{-l}, & 1 > |q_y| > e^{-zl} \\ e^{-l} < |q_\perp| < 0, & 1 > |q_y| > e^{-zl} \end{cases} \tag{8}$$

where the exponent  $z$  accounts for the anisotropy of the system. This blocking is very similar to the one used in [5].



The rescaling is anisotropic as well and is given by,

$$\begin{aligned} q'_\perp &= e^l q_\perp & h'(q') &= e^{-(D-1+z+\nu)l} h(q) \\ q'_y &= e^{z l} q_y & u'(q') &= e^{-(D-1+2\nu)l} u(q) , \end{aligned} \quad (9)$$

where  $\nu$  is the other exponent that appears in the theory.

The result of performing a renormalization group transformation up to time '1', is the Wilsonian free energy

$$F_l(u', \vec{h}') , \quad (10)$$

where the  $u'$  and  $\vec{h}'$  fields have the same range as the original ones. The free energy evaluated at  $l = 0$  is, by definition, Eq. 6.

For future reference, let us work out the simplest fixed point in Eq. 6, the Gaussian fixed point. Although this fixed point is not of direct physical interest it plays a central role in many considerations (see Fig. 2). This fixed point may be studied by retaining only the quadratic terms in the free energy Eq. 6, and applying the RG transformation just defined. We easily get (hereafter dropping all primes in the rescaling)

$$\begin{aligned} F_l &= \frac{1}{2} \int d^{D-1} \hat{q}_\perp d\hat{q}_y \left[ (e^{(D-1-3z+2\nu)l} \kappa q_y^4 + e^{(D-3+z+2\nu)l} t q_\perp^2) h(q) h(-q) \right. \\ &\quad \left. + (e^{(D-1-3z+4\nu)l} g_y q_y^2 + e^{(D-3-z+4\nu)l} g_\perp q_\perp^2) u(-q) u(q) \right] . \end{aligned} \quad (11)$$

Imposing that the Gaussian fixed point is given by the terms involving  $\vec{h}$ , the exponents  $z$  and  $\nu$  are readily computed to be

$$z = \frac{1}{2} , \quad 2\nu = \frac{5}{2} - D \quad (12)$$

and the exponents for the operators associated with the couplings are uniquely determined. The Gaussian fixed point is thus  $g_y = g_\perp = 0$ . The coupling  $g_\perp$  defines an irrelevant direction for  $D > 3/2$ , with exponent  $\frac{3}{2} - D$ , while  $g_y$  defines a relevant direction for  $D < 5/2$ , with exponent  $\frac{5}{2} - D$ . The Gaussian fixed point is therefore infrared unstable.

## 2.2 The rotations of the tubule

For the general free energy of Eq. 6 the rotations of the tubule are implemented by

$$\begin{aligned} u &\rightarrow u \cos \theta + \sin \theta h + (\cos \theta - 1) y \\ h &\rightarrow h \cos \theta - \sin \theta u - \sin \theta y \end{aligned} , \quad (13)$$

where we have simplified by rotating just one component of  $\vec{h}$ . The symmetry transformation above is unusual in that it changes under the action of the renormalization group. This happens because rotations of the tubule mix two sets of fields – the in-plane and out-of-plane phonons – having different scaling dimensions. In fact, it is straightforward to show that Eq. 13 is realized at time ‘1’ by

$$\begin{aligned} u &\rightarrow u \cos \theta + e^{-(\nu-z)l} h \sin \theta + e^{-2(\nu-z)l} (\cos \theta - 1) y \\ h &\rightarrow h \cos \theta - e^{(\nu-z)l} u \sin \theta - e^{-(\nu-z)l} \sin \theta y . \end{aligned} \quad (14)$$

The above transformation is an exact symmetry of the free energy Eq. 10. This transformation depends explicitly on  $l$  and prevents a simple construction of invariant free energies. At large  $l$ , however, we may derive an  $l$ -independent version. Define  $\theta = Ae^{(\nu-z)l}$  and assume that the condition

$$\nu(l) - z(l) < 0 \quad (15)$$

is satisfied. Near the fixed point, scaling relations to be derived later show that

$$\nu - z = \frac{1}{3}(\nu - D + 1) \quad (16)$$

and therefore  $\nu - z < 0$  for all  $\nu < D - 1$ . The physical case  $D = 2$  requires  $\nu < 1$ , which is always valid.

Eq. 14 is then, for large  $l$ ,

$$\begin{aligned} u &\rightarrow u + Ah - \frac{1}{2}A^2y + \mathcal{O}(e^{2(\nu-z)l}) \\ h &\rightarrow h - Ay + \mathcal{O}(e^{2(\nu-z)l}) . \end{aligned} \quad (17)$$

The generalization of this symmetry to an arbitrary rotation involving  $\vec{h}$  is

$$\begin{aligned} u &\rightarrow u + \vec{A}\vec{h} - \frac{1}{2}\vec{A}^2y + \mathcal{O}(e^{2(\nu-z)l}) \\ \vec{h} &\rightarrow \vec{h} - \vec{A}y + \mathcal{O}(e^{2(\nu-z)l}) , \end{aligned} \quad (18)$$

which is the tubular phase version of a symmetry noted earlier in [9] for the free energy describing the large distance properties of the flat phase.

### 2.3 The large distance free energy of the Phantom tubule

Let us apply the previous considerations to the construction of the free energy for the large distance properties of phantom tubules (Eq. 6 with  $b = 0$ ).

In [3, 5], the free energy

$$F(u, \vec{h}) = \frac{1}{2} \int d^{D-1} \mathbf{x}_\perp dy \left[ \kappa (\partial_y^2 \vec{h})^2 + t (\partial_\alpha \vec{h})^2 + g_\perp (\partial_\alpha u)^2 + g_y (\partial_y u + \frac{1}{2} (\partial_y \vec{h})^2)^2 \right], \quad (19)$$

is given as that describing the right large distance properties of the TP.

The first thing to notice is that this free energy is not invariant under the symmetry Eq. 18. The free energy with the correct invariances is given by

$$F(u, \vec{h}) = \frac{1}{2} \int d^{D-1} \mathbf{x}_\perp dy \left[ \kappa (\partial_y^2 \vec{h})^2 + t (\partial_\alpha \vec{h})^2 + g_\perp (\partial_\alpha u + \partial_\alpha \vec{h} \partial_y \vec{h})^2 + g_y (\partial_y u + \frac{1}{2} (\partial_y \vec{h})^2)^2 \right], \quad (20)$$

since the operator  $\partial_\alpha u + \partial_\alpha \vec{h} \partial_y \vec{h}$  is rotationally invariant.

It is important at this point to recall that the symmetry Eq. 18 is exact up to ‘irrelevant’ terms, and the coupling  $g_\perp$  is irrelevant for all the entire range of  $D$  (including  $D = 2$ ) in which the TP exists. If we therefore insist on including irrelevant operators around the Gaussian fixed point, our free energy would certainly contain a non-invariant term under Eq. 18,

$$F(u, \vec{h}) = \frac{1}{2} \int d^{D-1} \mathbf{x}_\perp dy \left[ \kappa (\partial_y^2 \vec{h})^2 + t (\partial_\alpha \vec{h})^2 + g_\perp^{(1)} (\partial_\alpha u + \partial_\alpha \vec{h} \partial_y \vec{h})^2 + g_\perp^{(2)} (\partial_\alpha u)^2 + g_y (\partial_y u + \frac{1}{2} (\partial_y \vec{h})^2)^2 \right]. \quad (21)$$

Indeed, this is the combination that appears, up to higher irrelevant terms, in the general expression for the free energy Eq. 6, as  $g_\perp^{(1)}$  is the coupling to the  $F_\alpha F^\alpha$  operator, and  $g_\perp^{(2)}$  is the coupling to  $F_\alpha^\alpha$ .

The usual strategy, nevertheless, is to keep just those operators that define relevant directions of the Gaussian fixed point. It is these directions that flow towards new infrared fixed points, unless a first order transition occurs. Adopting this approach the relevant free energy for the phantom tubule would be

$$F(u, \vec{h}) = \frac{1}{2} \int d^{D-1} \mathbf{x}_\perp dy \left[ \kappa (\partial_y^2 \vec{h})^2 + t (\partial_\alpha \vec{h})^2 \right]$$

$$+ g_y(\partial_y u + \frac{1}{2}(\partial_y \vec{h})^2)^2 \Big] , \quad (22)$$

where  $g_y$  defines a relevant direction for  $D < 5/2$  which terminates in the tubular phase fixed point (TPFP) as shown in Fig. 2. Note that the symmetry Eq. 18 is, indeed, preserved.

## 2.4 The large distance free energy for the self-avoiding tubule

Now let us return to the more physical model with the self-avoidance term,

$$\frac{b}{2} \int dy d^{D-1} \mathbf{x}_\perp \int dy' d^{D-1} \mathbf{x}'_\perp \delta^d(\vec{r}(\mathbf{x}_\perp, y) - \vec{r}(\mathbf{x}'_\perp, y')). \quad (23)$$

restored.

Following the discussion in subsection 2.2, we simplify the self-avoiding term Eq. 23 by demanding invariance under the symmetry Eq. 18,

$$\frac{b}{2} \int dy d^{D-1} \mathbf{x}_\perp d^{D-1} \mathbf{x}'_\perp \delta^{d-1}(\vec{h}(\mathbf{x}_\perp, y) - \vec{h}(\mathbf{x}'_\perp, y)) , \quad (24)$$

with irrelevant terms dropped.

The scaling dimension of the new perturbation Eq. 24 at the Gaussian fixed point is  $\varepsilon = 3D - \frac{1}{2} - (\frac{5}{2} - D)d$ . The  $b$  coupling therefore defines a new relevant direction for  $D$  tubules embedded in dimensions  $d < d_c^{SA}$ , where

$$d_c^{SA}(D) = \frac{6D - 1}{5 - 2D} . \quad (25)$$

Below the upper critical dimension  $d_c^{SA}$  the Gaussian fixed point is infrared unstable under this perturbation, and the large distance properties of the self-avoiding tubule are described by a new fixed point (SAFP). This new fixed point merges with the Gaussian fixed point at the upper critical dimension where self-avoidance becomes a marginal perturbation. We therefore expect the critical properties of the self-avoiding tubule to be perturbative in  $\varepsilon$ , as pointed out first in [6] (see Fig. 2).

In [5], however, it is claimed that this simple scenario is valid only for tubules embedded in dimensions  $d$  close to  $d_c^{SA}(D)$ . For any dimension  $d$  lower than  $d_*$  (where  $d_* < d_c^{SA}$ ), they argue for the existence of a distinct fixed

point, the bending rigidity fixed point (BRFP) (see Fig. 3). This fixed point is postulated to describe the actual critical properties of the self-avoiding tubule for the regime  $d < d_*$ , including the physical case of the  $D = 2$  tubule embedded in  $d = 3$ . If this scenario is true, the critical properties of the self-avoiding tubule are not perturbative in  $\varepsilon$ . Analytical predictions become then extremely difficult, as there is no evident small perturbative parameter.

At this stage, therefore, we need to understand better the topology of the RG flows in the case where self-avoidance is included. Let us review the arguments of [5]. They consider the free energy Eq. 19, together with the self-avoiding term Eq. 24. They include all relevant directions from the Gaussian fixed point, and an irrelevant one defined by  $g_\perp$ . They apply the infinitesimal renormalization group a la Wilson to derive an equation for the evolution of couplings. The crucial equation in their analysis is the RG flow equation for  $g_\perp$

$$\frac{dg_\perp}{dl} = [4\nu - z + D - 3] g_\perp . \quad (26)$$

Now, as the RG is iterated starting near the Gaussian fixed point,  $g_\perp$  decreases to zero while the rescalings  $\nu(l)$  and  $z(l)$  flow towards their SAFD values. For sufficiently small embedding dimension  $d$  and large enough  $l$  the sign of the  $\beta$ -function for  $g_\perp$  changes sign. The coupling  $g_\perp$  then flows to the BRFP  $g_\perp^* = \infty$  (see Fig. 3). This argument can be made more quantitative. Under very reasonable assumptions, Eq. 26 leads to a lower bound for  $d_*$ , the highest embedding dimension in which the BRFP prevails,

$$d_*(D) > \frac{4D - 1}{4 - D} . \quad (27)$$

In particular,  $d_*(2) > 7/2 > 3$ , so the physical tubule ( $D = 2, d = 3$ ) is, according to [5], described by the BRFP.

It is apparent that the operator

$$\partial_\alpha u \partial^\alpha u \quad (28)$$

plays a fundamental role in this argument. Let us examine it more closely. In an expansion in irrelevant operators around the Gaussian fixed point, it appears in two ways, which we labeled  $g_\perp^{(1)}$  and  $g_\perp^{(2)}$  in Eq. 21.

First of all, the operator associated to  $g_\perp^{(1)}$  is invariant under the symmetry Eq. 18, as it appears in the invariant combination

$$\partial_\alpha u + \partial_\alpha \vec{h} \partial_y \vec{h} . \quad (29)$$

In contrast  $g_{\perp}^{(2)}$  couples to a subdominant piece of the operator  $F_{\alpha}^{\alpha} \equiv \partial_{\alpha} u \partial^{\alpha} u + \partial_{\alpha} \vec{h} \partial^{\alpha} \vec{h}$  (see Eq. 5). In fact, from our earlier symmetry arguments, it is suppressed by a factor  $\mathcal{O}(e^{2(\nu-z)})$  with respect to the dominant piece  $(\partial_{\alpha} \vec{h})^2$  which couples to the marginal direction  $t$ . Provided  $\nu - z < 0$  the coupling  $g_{\perp}^{(2)}$  is thus irrelevant and may be dropped from the free energy.

We have argued that the most general free energy dictating the large distance properties of the tubule is given by Eq. 20 together with self-avoidance (Eq. 24). For  $g_{\perp}$  vanishing, the infrared stable fixed point of the theory is the SAFFP. The key issue is now whether this fixed point is stable with respect to perturbations by  $g_{\perp}$ . Since the properties of the SAFFP are perturbative in  $\varepsilon$ , the same applies to the critical exponents. Experience with typical multicritical behavior suggest that we should not expect the exponent associated with the  $g_{\perp}$  direction to change so much from its gaussian value  $3/2 - D$  that it changes sign [10].

In conclusion, the simplest free energy describing the large distance properties of the self-avoiding tubule is given by

$$F(u, \vec{h}) = \frac{1}{2} \int d^{D-1} \mathbf{x}_{\perp} dy \left[ \kappa (\partial_y^2 \vec{h})^2 + t (\partial_{\alpha} \vec{h})^2 + g_y (\partial_y u + \frac{1}{2} (\partial_y \vec{h})^2)^2 \right] + \frac{b}{2} \int dy d^{D-1} \mathbf{x}_{\perp} d^{D-1} \mathbf{x}'_{\perp} \delta^{d-1} (\vec{h}(\mathbf{x}_{\perp}, y) - \vec{h}(\mathbf{x}'_{\perp}, y)) . \quad (30)$$

This is the starting point of all our subsequent analysis.

### 3 The Scaling Relations

Having identified the right free energy, we turn now to the derivation of the different critical exponents of the theory. We use the conventional field theory formalism [10], following [6].

The scaling dimensions of the fields and coordinates are  $[y] = 1, [x_{\perp}] = 2, [\vec{h}] = \frac{5}{2} - D$  and  $[u] = 4 - 2D$ . This implies

$$[b] = -\varepsilon, [g_y] = 2D - 5, \quad (31)$$

with

$$\varepsilon = 3D - \frac{1}{2} - \frac{5 - 2D}{2} d. \quad (32)$$

Following the arguments in [6], one can show that the free energy Eq. 30 renormalizes onto itself with

$$\begin{aligned}
F(u, \vec{h}) &= \frac{1}{2} \int d^{D-1} \mathbf{x}_\perp^R dy \left[ Z \kappa (\partial_y^2 \vec{h}^R)^2 + Z_\perp t (\partial_\alpha^R \vec{h}^R)^2 \right. \\
&\quad \left. + g_y^R \mu^{-5+2D} (\partial_y u^R + \frac{1}{2} (\partial_y \vec{h}^R)^2)^2 \right] \\
&\quad + \frac{b^R Z_b \mu^\varepsilon}{2} \int d^{D-1} \mathbf{x}_\perp^R d^{D-1} \mathbf{x}'_\perp dy \delta^{d-1} (\vec{h}^R(\mathbf{x}_\perp^R, y) - \vec{h}^R(\mathbf{x}'_\perp, y)),
\end{aligned} \tag{33}$$

where the Ward identity implied by Eq. 18 is used so that there is no independent wave function renormalization for the field  $u$ . Furthermore, it is not difficult to show, using the MOPE formalism [12], that the bending rigidity is not renormalized so  $Z = 1$ , as first pointed out in [6]. Thus we have

$$\begin{aligned}
\vec{h}^R(\mathbf{x}_\perp^R, y) &= Z_\perp^{\frac{1-D}{4}} \vec{h}(\mathbf{x}_\perp, y) \\
\mathbf{x}_\perp^R &= Z_\perp^{\frac{1}{2}} \mathbf{x}_\perp \\
b^R &= b \mu^{-\varepsilon} Z_b^{-1} Z^{(1-D)\frac{d+3}{4}} \\
g_y^R &= \mu^{5-2D} g_y Z_\perp^{\frac{D-1}{2}} .
\end{aligned} \tag{34}$$

Using these definitions we will consider two correlators, which enable us to determine the exponents of the theory. In the original paper [6], the correlator

$$G_h(\mathbf{x}_\perp, y) \equiv -\frac{1}{2(d-1)} \langle (\vec{h}(\mathbf{x}_\perp, y) - \vec{h}(\mathbf{0}, 0))^2 \rangle \tag{35}$$

was considered as well the correlator involving the  $u$  fields,

$$G_u(\mathbf{x}_\perp, y) \equiv \langle \partial_y u(\mathbf{x}_\perp, y) \partial_y u(\mathbf{0}, 0) \rangle . \tag{36}$$

At the fixed point, the first correlator satisfies

$$\left\{ \mu \frac{\partial}{\partial \mu} + \frac{\delta}{2} \mathbf{x}_\perp \frac{\partial}{\partial \mathbf{x}_\perp} + \frac{D-1}{2} \delta \right\} G_h^R(\mathbf{x}_\perp, y) = 0 , \tag{37}$$

which, combined with simple scaling law

$$\left\{ \mu \frac{\partial}{\partial \mu} - y \frac{\partial}{\partial y} - 2 \mathbf{x}_\perp \frac{\partial}{\partial \mathbf{x}_\perp} + (5-2D) \right\} G_h^R(\mathbf{x}_\perp, y) = 0 , \tag{38}$$

gives us the fixed point renormalization group equation,

$$\left\{ y \frac{\partial}{\partial y} + \frac{1}{z} \mathbf{x}_\perp \frac{\partial}{\partial \mathbf{x}_\perp} - 2\zeta \right\} G_h^R(\mathbf{x}_\perp, y) = 0 . \quad (39)$$

A renormalization group equation may also be derived for  $G_u$ . To do so we must use once again the Ward identity that fixes the wave function renormalization for  $u$ . Eq. 37 is now,

$$\left\{ \mu \frac{\partial}{\partial \mu} + \frac{\delta}{2} \mathbf{x}_\perp \frac{\partial}{\partial \mathbf{x}_\perp} + (D-1)\delta \right\} G_u^R(\mathbf{x}_\perp, y) = 0 , \quad (40)$$

Eq 38 reads for the  $u$  case,

$$\left\{ \mu \frac{\partial}{\partial \mu} - y \frac{\partial}{\partial y} - 2\mathbf{x}_\perp \frac{\partial}{\partial \mathbf{x}_\perp} + (6-4D) \right\} G_u^R(\mathbf{x}_\perp, y) = 0 , \quad (41)$$

leading finally to

$$\left\{ y \frac{\partial}{\partial y} + \frac{1}{z} \mathbf{x}_\perp \frac{\partial}{\partial \mathbf{x}_\perp} - 2\zeta_u \right\} G_h^R(\mathbf{x}_\perp, y) = 0 , \quad (42)$$

where

$$\begin{aligned} \delta &= \mu \frac{d}{d\mu} \Big|_0 \log Z_\perp \\ z &= \frac{2}{4 + \delta} \\ \zeta &= \frac{5 - 2D}{2} + \frac{1 - D}{4} \delta \\ \zeta_u &= 1 + \frac{1 - D}{z} . \end{aligned} \quad (43)$$

Both, Eqs 39 and 42 may be solved explicitly, yielding

$$\begin{aligned} G_h(\mathbf{x}_\perp, y) &= y^{2\zeta} F_1\left(\frac{y}{|\mathbf{x}_\perp|^z}\right) = |\mathbf{x}_\perp|^\nu F_2\left(\frac{y}{|\mathbf{x}_\perp|^z}\right) \\ G_u(x_\perp, y) &= y^{2\zeta_u} F_1'\left(\frac{y}{|\mathbf{x}_\perp|^z}\right) = |\mathbf{x}_\perp|^{2\frac{\zeta_u}{z}} F_2'\left(\frac{y}{|\mathbf{x}_\perp|^z}\right) , \end{aligned} \quad (44)$$



where  $\nu = \frac{\zeta}{z}$ . Transforming Eq. 44 to momentum space gives

$$\begin{aligned} G_h(\mathbf{p}_\perp, q)^{-1} &= |\mathbf{p}_\perp|^{2+\eta_\perp} f\left(\frac{q}{|\mathbf{p}_\perp|}\right) \\ G_u(\mathbf{p}_\perp, q)^{-1} &= |\mathbf{p}_\perp|^{z\eta_u} h\left(\frac{q}{|\mathbf{p}_\perp|}\right) \end{aligned} \quad (45)$$

with

$$\begin{aligned} \eta_\perp &= -2 + 4z \\ \eta_u &= \frac{2\nu}{z} . \end{aligned} \quad (46)$$

These scaling laws were first derived in [6] and [3] respectively.

We conclude that all the critical exponents of our Free energy Eq. 30 at any putative fixed point may be expressed in terms of a single parameter, say  $\delta$ . The task of computing critical exponents translates into the task of evaluating  $\delta$  at the corresponding fixed point.

## 4 The Phantom tubule

The theoretical considerations in subsection 2.3 lead us to consider Eq. 22 as the right free energy describing the large distance properties of the phantom tubule. In fact they allow us to solve the phantom tubule phase exactly, simply by performing the shift

$$u \rightarrow u' - \frac{1}{2} \int_0^y dz (\partial_z \vec{h})^2 , \quad (47)$$

where the lower bound for the integral is arbitrary and corresponds to translations of the zero mode. The free energy Eq. 22 is then a sum of Gaussian terms. Let us compute the anomalous elasticity, determined by the correlator Eq. 36

$$G_u(\mathbf{x} - \mathbf{z}) = \langle \partial_y u(\mathbf{x}) \partial_y u(\mathbf{z}) \rangle , \quad G_u(\mathbf{p}) = \int d(\mathbf{x} - \mathbf{z}) e^{-\mathbf{p}(\mathbf{x} - \mathbf{z})} G(\mathbf{x} - \mathbf{z}) . \quad (48)$$

The elasticity constant is given by

$$g_y(\mathbf{p}) = \frac{1}{G_u(\mathbf{p})} . \quad (49)$$

At tree level  $g_y(\mathbf{p}) = g_y$ .

The general case amounts to performing the shift Eq. 47. Equivalently the loop expansion may be performed to all orders. The diagrams consists of a necklace of  $\vec{h}$  loops which can be resummed, yielding

$$\begin{aligned} \frac{1}{g_y(\mathbf{p})} &= \frac{1}{g_y} + \frac{d-1}{2} \int d^{D-1} \hat{\mathbf{q}}_{\perp} d\hat{q}_y \frac{q_y^2 (p-q)_y^2}{(\kappa q_y^4 + t q_{\perp}^2)(\kappa(q_y - p_y)^4 + t(\mathbf{q}_{\perp} - \mathbf{p}_{\perp})^2)} \\ &+ \left( \frac{d-1}{2} \int d^{D-1} \hat{\mathbf{q}}_{\perp} d\hat{q}_y \frac{q_y^2}{\kappa(q_y^2)^2 + t \mathbf{q}_{\perp}^2} \right)^2 \delta(\mathbf{p}) , \end{aligned} \quad (50)$$

which for  $\mathbf{p} \neq 0$  is

$$g_y(\mathbf{p}) = \frac{g_y}{1 + \frac{(d-1)g_y}{2t^2} f(D-1) p_y^{2D-5} C\left(\frac{p_y}{|\mathbf{p}_{\perp}|^z}\right)} , \quad (51)$$

where  $f(d) = \int d^d \hat{t} \frac{1}{(t^2+1)^4}$ ,

$$C(y) = \int_{-\infty}^{+\infty} d\hat{z} \int_0^1 dx \left( \frac{x(1-x)}{y^4} + \frac{\kappa}{t} (x(1-z)^4 + (1-x)z^4) \right)^{\frac{D-5}{2}} , \quad (52)$$

and the exponent  $z$  is

$$z = 1/2 . \quad (53)$$

Recall that Eq. 51 is valid for any value of  $g_y$ . The Gaussian fixed point ( $g_y = 0$ ) is unstable to perturbations along this direction, and the coupling  $g_y$  is driven to  $g_y = \infty$  in the infrared, which is the fixed point describing the physics of the phantom tubule (PTFP). At the PTFP  $g_y(\mathbf{p})$  has the form  $p_y^{\eta_u} g\left(\frac{p_y}{|\mathbf{p}_{\perp}|^z}\right)$ , as predicted by Eq. 44 at any fixed point.

We can easily recover now the results in [3, 5] from our exact solution Eq. 51 and Eq. 52 at the PTFP:

- For  $y \equiv \frac{p_y}{|\mathbf{p}_{\perp}|^z} \rightarrow \infty$

we have

$$C(y)_{y \rightarrow \infty} \sim \left(\frac{\kappa}{t}\right)^{\frac{D-5}{2}} \frac{2}{D-3} \int_{-\infty}^{+\infty} d\hat{z} z^2 (1-z)^2 \frac{(1-z)^{2(D-3)} - z^{2(D-3)}}{(1-z)^4 - z^4} \quad (54)$$

which converges, both in the infrared and the ultraviolet for  $\frac{3}{2} < D < \frac{5}{2}$  (the dimensions in which the tubular phase exists). For small  $p_y$

$$g_y(\mathbf{p}) \sim p_y^{\eta_u} , \quad \eta_u = 5 - 2D. \quad (55)$$

- For  $y \equiv \frac{p_y}{|\mathbf{p}_\perp|^z} \rightarrow 0$   
we have

$$C(y)_{y \rightarrow 0} \sim \frac{y^{-2D+5}}{2} \left(\frac{t}{\kappa}\right)^D \int_0^1 (x(1-x))^{\frac{2D-5}{2}} \int_0^{+\infty} d\hat{z} z^{1/4} (1+z)^{\frac{D-5}{2}} \quad (56)$$

so  $C(y)_{y \rightarrow 0} \sim y^{\eta_u} \text{Const.}$  where  $\text{Const.}$  is a convergent integral for  $\frac{3}{2} < D < \frac{5}{2}$ . For small  $p_\perp$  at  $D = 2$

$$g_y(\mathbf{p}) \sim p_\perp^{1/2} . \quad (57)$$

To conclude let us connect with the results in section 3. At the PTFP we have  $\delta = 0$ , and rest of the exponents from this result and scaling relations.

## 5 The self-avoiding tubule

We have argued that Eq. 30 is the appropriate free energy to consider once self-avoidance is included. The task of computing the critical exponents of this theory is not easy, since from [6] we know that the results of the  $\varepsilon(d)$ -expansion are not very robust to higher order perturbations.

In order to get an estimate for the exponents at the SAFFP, we compute the critical exponents to lowest order in  $\varepsilon(D, d)$  for arbitrary internal dimension  $D$ . Existing techniques [13, 14] then allow us to perform more sophisticated extrapolations which produce reliable estimates for the critical exponents.

### 5.1 The computation of $\delta$

We follow the MOPE formalism [12], employing dimensional regularization and minimal subtraction, used first in this problem in [6], to compute the  $\delta$  exponent.

Within the MOPE formalism, one may prove that the free energy Eq. 30 renormalizes onto itself. It also identifies the diagrams to compute that yield the RG functions determining the critical exponents. For details on this formalism we refer to [11, 12], and for its implementation in the tubular case, we refer to the original BG [6] calculation.

The first step is to compute the two-point function  $G_h$  for arbitrary  $D$  at  $b = 0$ . The result is

$$G_h^0(\mathbf{x}_\perp, y) = -\frac{|\mathbf{x}_\perp|^{2-D}}{(\frac{5}{2}-D)(2\pi)^{\frac{D+1}{2}}} \left[ |\mathbf{x}_\perp|^{\frac{1}{2}} \int_0^{+\infty} dt t^{\frac{D}{2}-1} K_{\frac{1-D}{2}}(t) \cos(t^{\frac{1}{2}} w) + \frac{y}{2} \int_0^{+\infty} dt t^{\frac{D-3}{2}} K_{\frac{3-D}{2}}(t) \sin(t^{\frac{1}{2}} w) \right] \quad (58)$$

where  $w = \frac{y}{|\mathbf{x}_\perp|^{\frac{1}{2}}}$  and  $K_\nu$  is a modified Bessel function. There are two particular cases of interest. At  $y = 0$  we have

$$G_h^0(\mathbf{x}_\perp, 0) = -\frac{|\mathbf{x}_\perp|^{\frac{5}{2}-D} \Gamma(\frac{1}{4}) \Gamma(\frac{D}{2} - \frac{1}{4})}{(\frac{5}{2}-D) \pi^{\frac{D+1}{2}} 2^{\frac{5}{2}}} . \quad (59)$$

For the physical value  $D = 2$  it follows from  $K_{\frac{1}{2}}(t) = K_{-\frac{1}{2}}(t) = \left(\frac{\pi}{2t}\right)^{1/2} e^{-t}$ , that

$$G_h^0(x, y) = -\frac{|x|^{\frac{1}{2}}}{2\pi^{\frac{1}{2}}} e^{-\frac{w^2}{4}} - \frac{y}{4} \operatorname{erf}\left(\frac{w}{2}\right) , \quad (60)$$

where  $\operatorname{erf}(x)$  denotes the error function. This result is in complete agreement with that quoted in [6]. The next step is to perform the MOPE for the operator

$$\phi\{\mathbf{x}_\perp, \mathbf{x}'_\perp, y\} = \delta^{(d-1)}(\vec{h}(\mathbf{x}_\perp, y) - \vec{h}(\mathbf{x}'_\perp, y)) . \quad (61)$$

This is easily done using standard techniques, with the result

$$\phi\{\mathbf{x}_\perp, \mathbf{x}'_\perp, y\} = C_\phi^1(\mathbf{x}_\perp - \mathbf{x}'_\perp) + C_\phi^{\alpha\beta}(\mathbf{x}_\perp - \mathbf{x}'_\perp) : \nabla_\alpha \vec{h}(\mathbf{x}_\perp^0, y) \nabla_\beta \vec{h}(\mathbf{x}_\perp^0, y) : + \dots , \quad (62)$$

where  $\mathbf{x}_\perp^0 = \frac{\mathbf{x}_\perp + \mathbf{x}'_\perp}{2}$ , and the Wilson coefficients are

$$C_\phi(\mathbf{u}) = \frac{1}{(4\pi)^{\frac{d-1}{2}} (-G_h^0(\mathbf{u}, 0))^{\frac{d-1}{2}}} , \quad C_\phi^{\alpha\beta}(\mathbf{u}) = -\frac{u^\alpha u^\beta}{4(4\pi)^{\frac{d-1}{2}} (-G_h^0(\mathbf{u}, 0))^{\frac{d+1}{2}}} . \quad (63)$$

We also need the MOPE for the product of two of these operators. One finds

$$\phi\{\mathbf{x}_1^\perp, \mathbf{z}_1^\perp, y_1\} \phi\{\mathbf{x}_2^\perp, \mathbf{z}_2^\perp, y_2\} = C_{\phi\phi}^\phi(\mathbf{x}_1^\perp - \mathbf{x}_2^\perp, \mathbf{z}_1^\perp - \mathbf{z}_2^\perp, y_1 - y_2) \phi\{\mathbf{x}_\perp, \mathbf{z}_\perp, y\} + \dots , \quad (64)$$

where  $\mathbf{x}_\perp = \frac{\mathbf{x}_1^\perp + \mathbf{x}_2^\perp}{2}$ ,  $y = \frac{y_1 + y_2}{2}$  and  $\mathbf{z}_\perp = \frac{\mathbf{z}_1^\perp + \mathbf{z}_2^\perp}{2}$  and

$$C_{\phi\phi}^\phi(\mathbf{u}, \mathbf{v}, w) = \frac{1}{(4\pi)^{\frac{d-1}{2}}} \frac{1}{(-G_h^0(\mathbf{u}, w) - G_h^0(\mathbf{v}, w))^{\frac{d-1}{2}}}. \quad (65)$$

This is all we need to compute the critical exponents. This MOPE corresponds to the diagrams in Fig. 4. The last diagram for the renormalization of  $b$  is not necessary to compute, as it cancels against the renormalization of  $Z_\perp$ .

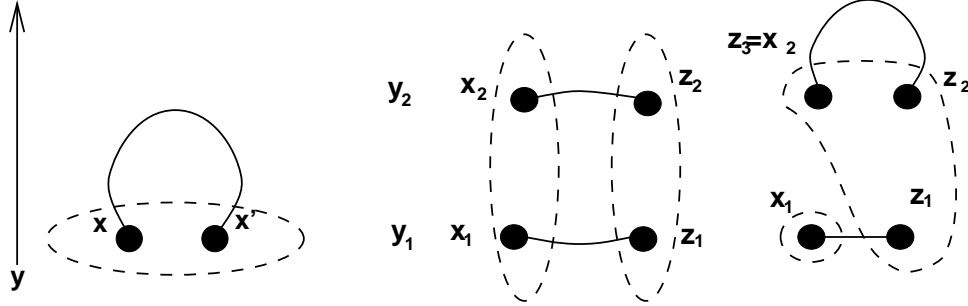


Figure 4: One loop diagrams contributing to the renormalization of the free energy.

Expanding the renormalized action Eq. 33, and using the MOPE Eq. 62,

$$\begin{aligned} & -\frac{b^R \mu^\varepsilon}{2} \int d^{D-1} \mathbf{x}_\perp d^{D-1} \mathbf{x}'_\perp dy \phi\{\mathbf{x}_\perp, \mathbf{x}'_\perp, y\} = \\ & -\frac{b^R \mu^\varepsilon}{2} \left( \int d^{D-1} \mathbf{x}_\perp d^{D-1} \mathbf{x}'_\perp dy C_\phi^1(\mathbf{x}_\perp - \mathbf{x}'_\perp) + \right. \\ & \left. + \int d^{D-1} \mathbf{x}_\perp d^{D-1} \mathbf{x}'_\perp dy C_\phi^{\alpha,\beta}(\mathbf{x}_\perp - \mathbf{x}'_\perp) \nabla_\alpha \vec{h}(\mathbf{x}_\perp^0, y) \nabla_\beta \vec{h}(\mathbf{x}'_\perp^0, y) + \dots \right). \end{aligned} \quad (66)$$

The first term of Eq. 66 renormalizes the identity operator and therefore may be neglected in computing expectation values of operators. The second term determines  $Z_\perp$ , with the result,

$$Z_\perp = 1 + \frac{1}{D-1} \left( \frac{5}{2} - D \right)^{\frac{2D+2}{5-2D}} \frac{\pi^{\frac{3D+3}{10-4D}} 2^{\frac{11-3D}{5-2D}}}{\left( \Gamma(\frac{1}{4}) \Gamma(\frac{D}{2} - \frac{1}{4}) \right)^{\frac{2D+2}{5-2D}}} \frac{b^R}{\Gamma(\frac{D-1}{2})} \frac{1}{\varepsilon}. \quad (67)$$

At one loop there is no renormalization for  $Z$ , a result that is also true at any order in perturbation theory [6].

Expanding the  $\delta$ -function, and performing the MOPE in Eq. 64, we find

$$\begin{aligned} & \frac{(b^R \mu^\varepsilon)^2}{8} \int d^{D-1} \mathbf{x}_\perp^0 d^{D-1} \mathbf{x}_\perp^{0'} dy_0 \delta^{d-1}(\vec{h}(\mathbf{x}_\perp^0, y_0) - \vec{h}(\mathbf{x}_\perp^{0'}, y_0)) \\ & \times \int d^{D-1} \mathbf{z} d^{D-1} \mathbf{w} dy C_{\phi\phi}^\phi(\mathbf{z}, \mathbf{w}, y), \end{aligned} \quad (68)$$

where higher terms in the MOPE Eq. 64 are neglected as they do not give rise to poles in  $\varepsilon$ . To find  $Z_b$ , we must compute the last integral in Eq. 68. This is done by performing the angular integration and then changing variables to  $u = \frac{|\mathbf{z}|^{1/2}}{y}$  and  $v = \frac{|\mathbf{w}|^{1/2}}{y}$ . The result is

$$\begin{aligned} \int d^{D-1} \mathbf{z} d^{D-1} \mathbf{w} dy C_{\phi\phi}^\phi(\mathbf{z}, \mathbf{w}, y) &= \frac{8}{(4\pi)^{\frac{d-1}{2}}} \left( \frac{2\pi^{\frac{D-1}{2}}}{\Gamma(\frac{D-1}{2})} \right)^{\frac{d-1}{2}} \\ &\times \left( \left( \frac{5}{2} - D \right) (2\pi)^{\frac{D+1}{2}} \right)^{\frac{d-1}{2}} \int_0^{\frac{1}{\mu}} dy y^{\varepsilon-1} \\ &\times \int_0^{\frac{1}{\mu y}} du \int_0^{\frac{1}{\mu y}} dv \frac{u^{2D-3} v^{2D-3}}{(f(u) + f(v))^{\frac{d-1}{2}}}, \end{aligned} \quad (69)$$

where

$$\begin{aligned} f(u) &= u^{4-2D} \left\{ u \int_0^{+\infty} dt t^{\frac{D}{2}-1} K_{\frac{1-D}{2}}(t) \cos\left(\frac{t^{1/2}}{u}\right) \right. \\ &\quad \left. + \frac{1}{2} \int_0^{+\infty} dt t^{\frac{D-2}{2}} K_{\frac{3-D}{2}}(t) \sin\left(\frac{t^{1/2}}{u}\right) \right\}. \end{aligned} \quad (70)$$

Using

$$\begin{aligned} & \int_0^{\frac{1}{\mu y}} du \int_0^{\frac{1}{\mu y}} dv \frac{u^{2D-3} v^{2D-3}}{(f(u) + f(v))^{\frac{d-1}{2}}} \\ &= \int_0^{+\infty} du \int_0^{+\infty} dv \frac{u^{2D-3} v^{2D-3}}{(f(u) + f(v))^{\frac{d-1}{2}}} + \rho(y), \end{aligned} \quad (71)$$

where  $\rho(y)$  is a continuous function that vanishes at  $y = 0$ , and adding a factor of 2 corresponding to the two ways one can perform the MOPE in the

diagram in Fig. 4, we get finally

$$Z_b = 1 + \frac{\left(\frac{5}{2} - D\right)^{\frac{4D-3}{5-2D}} 2^{\frac{(4D-3)(D-3)+4}{2(5-2D)}} I(D) \frac{b^R}{\varepsilon}}{\pi^{\frac{-7(D-1)}{2(5-2D)}} \Gamma\left(\frac{D-1}{2}\right)^2}, \quad (72)$$

with

$$I(D) = \int_0^{+\infty} du \int_0^{+\infty} dv \frac{u^{2D-3} v^{2D-3}}{(f(u) + f(v))^{\frac{4D-3}{5-2D}}}. \quad (73)$$

We have thus succeeded in renormalizing the theory at the one loop level. The evaluation of this integral is discussed in the Appendix. The next step is to compute the exponent  $\delta$ . We begin with the computation of the  $\beta$  function. There are two of them. Defining  $a_1$  and  $b_1$  via  $Z_{\perp} = 1 + \frac{b^R}{\varepsilon} a_1$  and  $Z_b = 1 + \frac{b^R}{\varepsilon} b_1$ , we have

$$\beta_b(b^R) = -\varepsilon b^R + \left(a_1 + \frac{7-\varepsilon}{2(5-2D)} b_1\right) (b^R)^2, \quad (74)$$

and

$$\beta_{g_y}(b^R, g_y^R) = \left(5 - 2D + \frac{D-1}{2} \Delta(b^R)\right) g_y^R, \quad (75)$$

where  $\Delta(b^R) = \mu \frac{d}{d\mu} \log Z_{\perp}$ . There is a nontrivial fixed point (the SAFP) at

$$b^{R*} = \frac{\varepsilon}{a_1 + \frac{7-\varepsilon}{2(5-2D)} b_1}, \quad (76)$$

and, for  $D < \frac{5-\Delta(b^{R*})/2}{2-\Delta(b^{R*})/2}$

$$g_y^R = +\infty. \quad (77)$$

Using

$$\delta = \Delta(b^{R*}) = \mu \frac{d}{d\mu} \log Z_{\perp} \Big|_{b^R=b^{R*}} \quad (78)$$

we obtain the final result

$$\delta = -\frac{\varepsilon}{\frac{7}{2(5-2D)} + \frac{a_1}{b_1}}. \quad (79)$$

Plugging Eq. 67 and Eq. 72 into Eq. 79 yields

$$\delta = -\frac{\left(\frac{5}{2} - D\right)}{\frac{7}{4} + \vartheta(D) I(D)} \varepsilon, \quad (80)$$

where

$$\vartheta(D) = (D - 1) \frac{(\Gamma(\frac{1}{4})\Gamma(\frac{D}{2} - \frac{1}{4}))^{\frac{2D+2}{5-2D}} 2^{\frac{2D^2-25D/2+27/2}{5-2D}}}{\pi\Gamma(\frac{D-1}{2})} . \quad (81)$$

The scaling relations after Eq. 42 and Eq. 46 determine the rest of the critical exponents provided we have a good determination of  $\delta$ . As only the first term in the  $\varepsilon$  expansion is available this will require refined methods to improve the perturbative expansion. This is an involved subject to which we now turn.

## 5.2 Analysis of the results

From Eq. 80 and the scaling relations we get explicit forms for the critical exponents of the self-avoiding tubular phase. For example, the radius of gyration or size exponent  $\nu$  reads,

$$\nu(D) = \frac{5 - 2D}{4} + \nu_1(D)\varepsilon(D, d) + \dots , \quad (82)$$

where  $\nu_1(D)$  is plotted as a function of  $D$  in Fig. 5.

As already noticed in [6], a direct application of Eq. 82 to a physical membrane is not robust with respect to second order corrections. This is a consequence of the point  $(D = 2, d = 3)$  being too far from the point  $(2, 11)$  on the critical curve  $\varepsilon = 0$ . One can try, instead, to perform a generalized  $\varepsilon$  expansion around any other point on the critical curve  $(D_0, d_0 = \frac{6D_0-1}{5-2D_0})$  (see Fig. 6) and hope to find a new expansion in which the corrections to Eq. 82 are minimized. In this case one may expect reliable one loop results.

As an example, let us rewrite Eq. 82 in terms of  $D - D_0$ , and keep the leading terms,

$$\begin{aligned} \nu(D) &= \frac{5 - 2D_0}{4} - \frac{D - D_0}{2} + \nu_1(D_0 + D - D_0)\varepsilon(D, d) + \mathcal{O}(\varepsilon^2) \\ &= \frac{5 - 2D_0}{4} - \frac{D - D_0}{2} + \nu_1(D_0)\varepsilon(D, d) \\ &\quad + \mathcal{O}(\varepsilon^2, \varepsilon(D - D_0), (D - D_0)^2) . \end{aligned} \quad (83)$$

One can expand around any point  $(D_0, d_0)$  in the  $\varepsilon = 0$  curve, but at the expense of dealing with the double expansion in  $\varepsilon$  and  $D$  in Eq. 83.



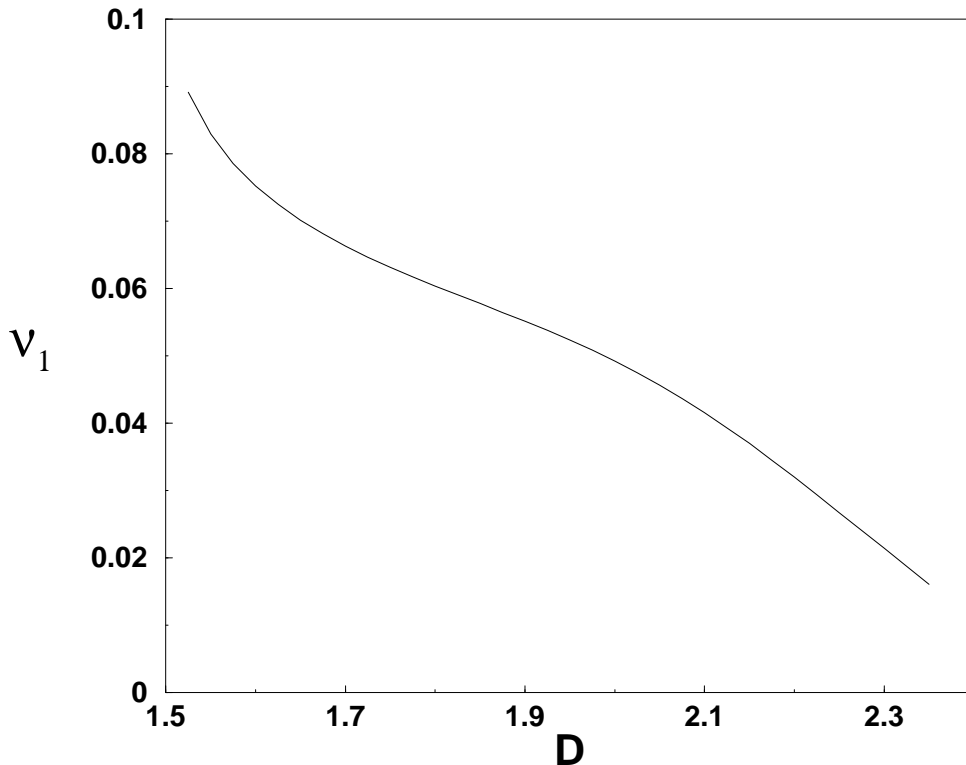


Figure 5: Plot of  $\nu_1(D)$  as a function of  $D$ .

Furthermore, critical quantities depend, in principle, on a new parameter  $D_0$ , but should obviously be independent of it. There are established techniques to select the best  $D_0$ , such as the minimal sensitivity method of Hwa [13]. Anyway, the expansion in  $\varepsilon, D$  is just a particular case of a more general situation [14], as we may choose any new set of variables  $\{x(D, \varepsilon), y(D, \varepsilon)\}$  and re-express Eq. 83 as an expansion around the critical curve  $(x_0 = x(D_0, 0), y_0 = y(D_0, 0))$ ,

$$\nu(D, \varepsilon) = \nu(x, y) = \nu(x_0, y_0) + \Delta x \nu_{1,0}(x_0, y_0) + \Delta y \nu_{0,1}(x_0, y_0) + \dots \quad (84)$$

where  $\Delta x = x(D, \varepsilon) - x_0$ ,  $\Delta y = y(D, \varepsilon) - y_0$ .

Now the goal is to choose a good set of variables  $\{x, y\}$  from the infinite number of possibilities.

A good expansion variable must meet two basic requirements;

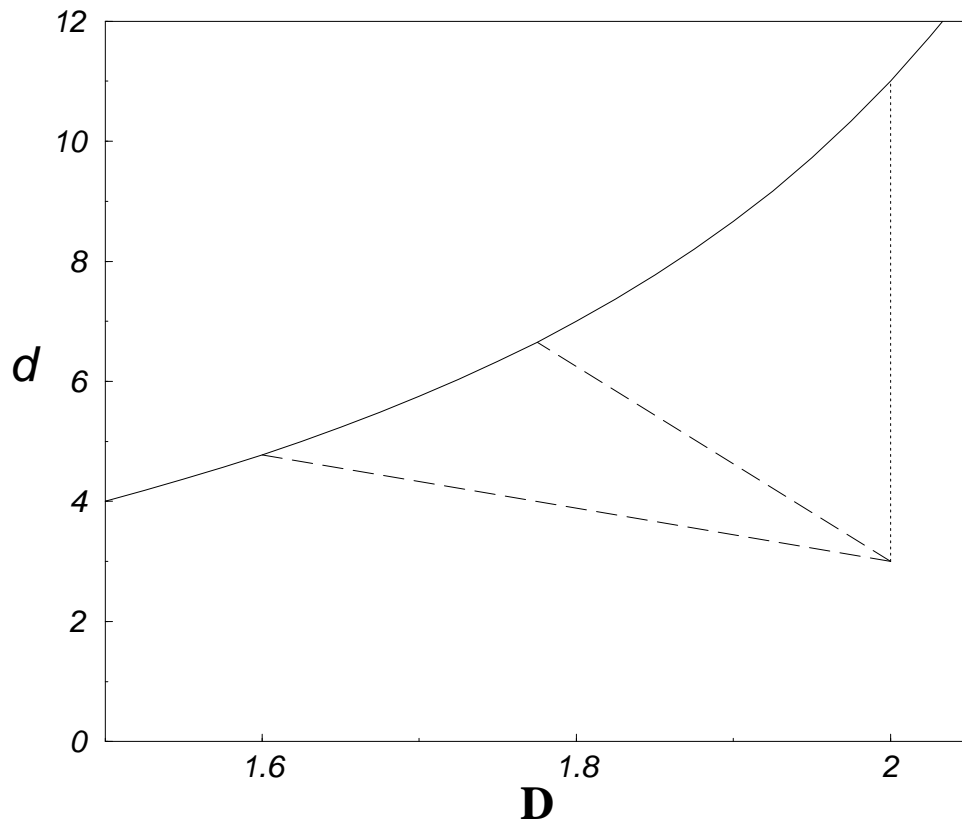


Figure 6: The solid line is the  $\varepsilon = 0$  curve. The naive  $\varepsilon$  expansion is marked with a dotted line. Other possible expansions from the physical interesting case ( $D = 2, d = 3$ ), are marked with dashed lines.

1. Independence of  $D_0$ , at least in some interval of  $D_0$ s.
2. Within this region, results must be quantitatively correct.

The way we choose to meet requirement 1, is to look for  $\nu$  to plateau within some given accuracy for an interval of  $D_0$ . To meet requirement 2, we will systematically study the  $(2, d)$  line, starting close to the  $d = 11$  where even the naive  $\varepsilon$  expansion is expected to work and agree well with the Flory estimate. At large  $d$  a good expansion variable should exhibit a broad plateau around the Flory result. At this stage, the expansions that do not deliver accurate enough results cannot be trusted, and should therefore be rejected. As  $d$  is decreased we check that the plateau remains stable for the good expansion variables, so that we have a reliable extrapolation at  $d = 3$ . In addition, we expect reasonable agreement with the Flory estimate.

We examine the  $\nu$  exponent as well as the  $\zeta$  exponent using the above techniques. The reason for analyzing both exponents is that they have different dependencies on  $\delta$ , as expressed in Eq. 43. This may result in different expansion variables being appropriate for different exponents. Of course, results must be consistent with the scaling relations expressed by Eq. 43.

In this paper, we implement Hwa minimal sensitivity scheme [13], and we explore the following distinct expansions;

- expansion A:  $\{x = D, y = \varepsilon\}$ .
- expansion B:  $\{x = D, y = d\}$ .
- expansion C:  $\{x = D, y = D_0(d) = \frac{5d+1}{2(3+d)}\}$ .
- expansion D:  $\{x = \varepsilon, y = D_0(d)\}$ .

which have been previously used in a different context in [14].

### 5.2.1 Corrections to mean field

The analysis leading to the extrapolation for the  $\nu$  exponent, may be summarized in Fig. 7. At  $(D = 2, d = 8)$  all sets of variables A,B,C,D give consistent results. Nevertheless, the expansion D shows the flattest plateau which is in complete agreement with the Flory estimate. This singles out expansion D as the best, and in fact we have taken as the actual  $\nu$  its value

at the middle of the plateau. Within the D expansion, results are largely independent of  $D_0$ . This allows us to estimate the uncertainty in  $\nu$  from its deviations from the plateau, which is the error bar quoted in the first column of Table 1. Expansion C also yields compatible results but, as apparent, it is not such a flat plateau. We find expansion B to be unreliable and the results are not even displayed. Finally, expansion A, almost equivalent to the naive  $\varepsilon$  expansion, shows a plateau coincident with D, but deviating slightly. The Hwa technique shows two extrema, one slightly above the Flory result, the other slightly below, so although the results are reasonable, we think we cannot apply it accurately as  $d$  decreases. At  $(2, 7)$ , the situation for the different extrapolations is very similar; again, expansion D gives a nice flat plateau consistent with the Flory estimate, and we extrapolate the best  $\nu$  in the same way as in the  $(2, 8)$  case. Expansion C gives a result completely consistent with D, although with not such a flat plateau, while expansion A starts to deviate. The cases  $(2, 6)$ ,  $(2, 5)$  and  $(2, 4)$  follow the same trends as the previous ones, as apparent from Fig. 7 and the results are quoted in Table 1. We conclude that expansion D is a reliable generalized  $\varepsilon$  expansion that we can confidently apply to the physical case  $(2, 3)$ . Our final result is quoted in Table 1. Let us recall that in [14] expansion D also gave the most reliable results, and it is interesting to find the same situation here.

Concerning the  $\zeta$  exponent, the situation is different. We find the best results applying Hwa's technique. For small  $d$  any of the estimates A,B,C,D exhibits a large enough plateau, and consequently, we are not confident enough of their robustness. The estimates quoted in Table 1 are those obtained from the Hwa method. As shown in Fig. 8 we find two points where  $\frac{\partial \nu}{\partial D_0} = 0$ , one for  $D_0 < 2$  the other for  $D_0 > 2$ . Our actual estimate corresponds to the case  $D_0 < 2$  since, on one hand it agrees slightly better with the Flory estimate for large  $d$ , and on the other the curve  $\varepsilon = 0$  seems intuitively closer to the actual point.

Finally, it is reassuring that the values we obtain for  $\nu$  and  $\zeta$ , although computed using different extrapolations, are compatible with the scaling relations Eq. 43.

### 5.2.2 Corrections to the Flory estimate

The Flory approximation, which certainly works well for polymers, also provides valuable insight in the case of membranes. The basic approximation

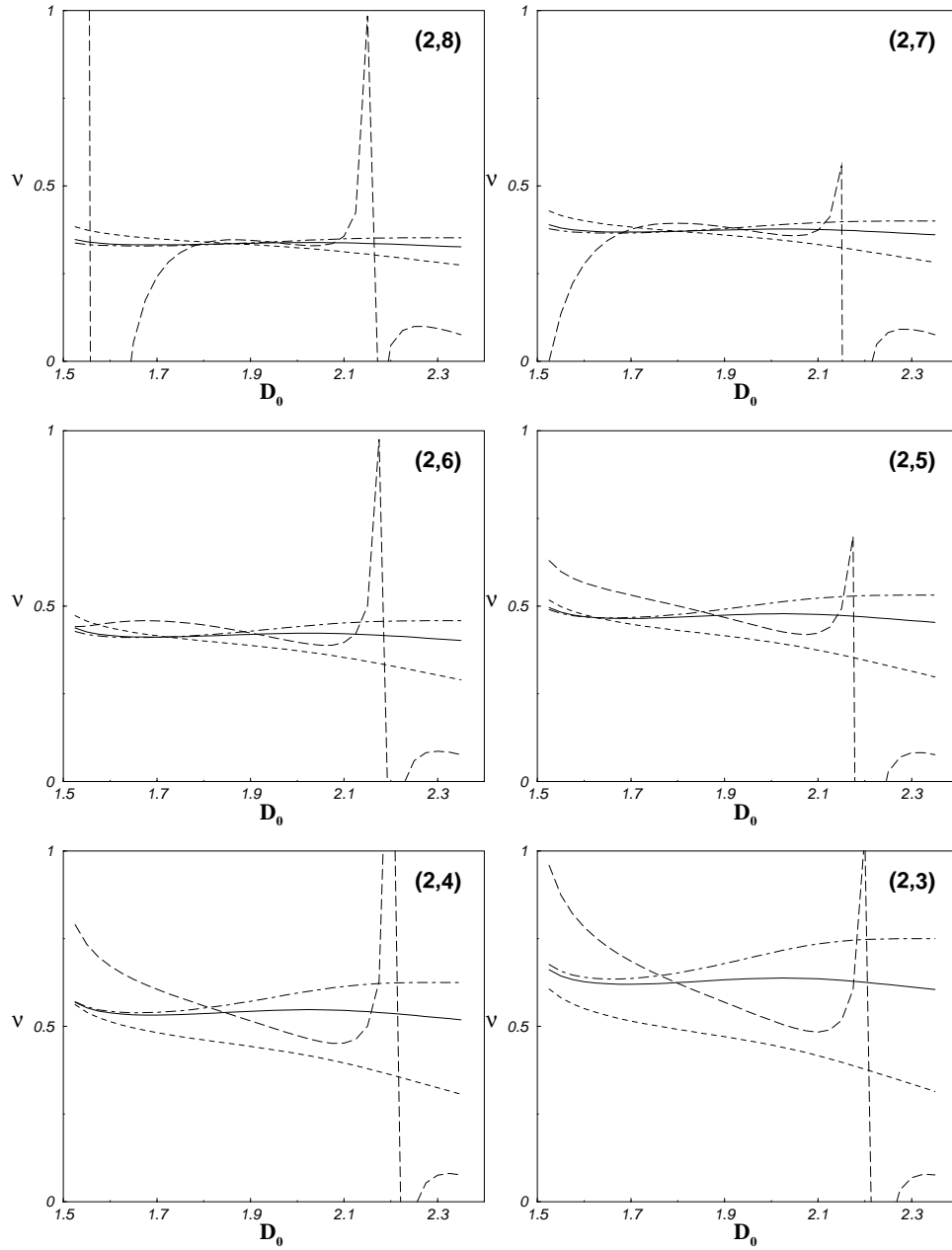


Figure 7: Calculation for the  $\nu$  exponent. The Long dashed line corresponds to the minimal sensitivity scheme, the dashed one is A expansion, dot-dashed corresponds to expansion C and the solid line is the D expansion.

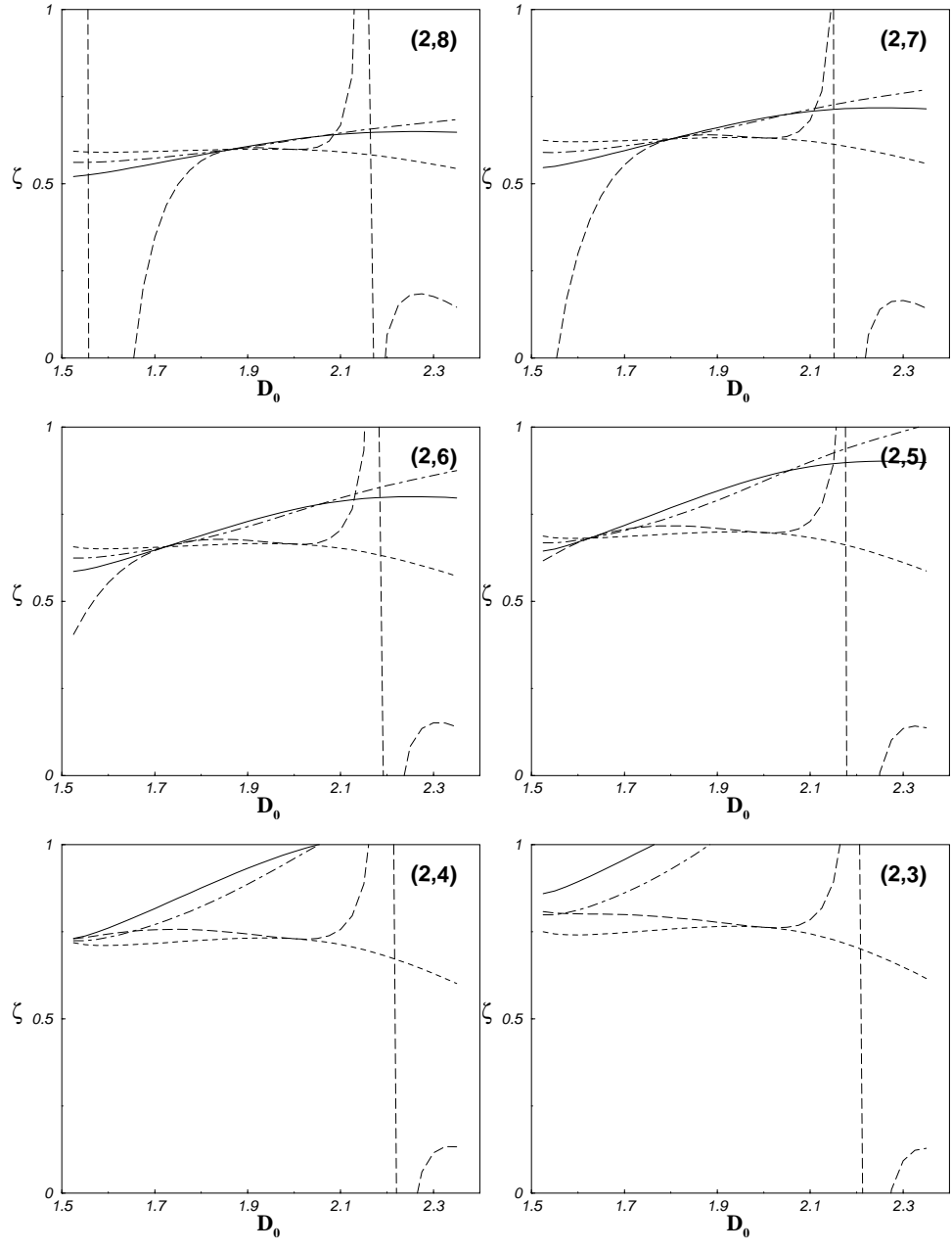


Figure 8: Calculation for the  $\zeta$  exponent. The conventions are the same as in the previous figure.

$d$	$\nu$	$\nu_{Flory}$	$\zeta$	$\zeta_{Flory}$
8	0.333(5)	0.333	0.60	0.600
7	0.374(8)	0.375	0.64	0.643
6	0.42(1)	0.429	0.68	0.692
5	0.47(1)	0.500	0.72	0.750
4	0.54(2)	0.600	0.76	0.818
3	0.62(2)	0.750	0.80	0.900

Table 1: Final results for critical exponents.

assumes that elastic energies are comparable to self-avoiding energies. For self-consistency we then require that  $Z_{\perp} = Z_b$ . This extra condition fixes  $\delta$  and  $\nu$  to be

$$\begin{aligned}\delta_F &= \frac{-4\varepsilon}{4 + (D - 1)(d + 3)} \\ \nu_{Flory} &= \frac{D + 1}{d + 1}.\end{aligned}\tag{85}$$

It is also interesting to analyze the corrections to the Flory result. We can write at the fixed point the following equivalent definition for  $\delta$ ,

$$\delta = \delta_F - \frac{4}{4 + (D - 1)(d + 3)} \mu \frac{d}{d\mu} \log\left(\frac{Z_b}{Z_{\perp}}\right).\tag{86}$$

Expanding to first order in  $\varepsilon$  it follows that

$$\nu_F(D) = \frac{5 - 2D}{4} + \frac{17 - 4D}{3(D + 1)} \nu_1(D) \varepsilon,\tag{87}$$

where  $\nu_1(D)$  is defined in Eq. 82. Coincidentally the extra factor appearing on the r.h.s of the previous equation is just 1 at  $D = 2$ , so Eq. 82 and Eq. 87 give the same result at  $D = 2$ , a result already noticed in [6].

We can apply the usual machinery to extract critical exponents. We start by examining the (2, 8) case. From Fig. 9 it is clear that all expansions give compatible results, although expansion C produces the flattest plateau. We use this expansion to extract our best  $\nu$  within this approximation. Using the fluctuations in the plateau, as a function of  $D_0$ , to estimate errors, we realize that results in this case are not as accurate, although still compatible

with previous estimates and with its Flory value. From analyzing this case we see also that this expansion tends to give a slight overestimate. The same situation holds as  $d$  decreases, as shown in Table 2. Overall, results remain close to the Flory estimate although with a larger uncertainty. They are still compatible with the values quoted in Table 1, which we regard as our most accurate determinations.

$d$	$\nu$	$\nu_F$	$\nu_V$	$\nu_{Flory}$
8	0.333(5)	0.34(1)	0.34(1)	0.333
7	0.374(8)	0.39(2)	0.39(2)	0.375
6	0.42(1)	0.44(2)	0.44(4)	0.429
5	0.47(1)	0.51(3)	0.51(5)	0.500
4	0.54(2)	0.60(4)	0.60(6)	0.600
3	0.62(2)	0.71(6)	0.70(9)	0.750

Table 2: Comparison of the different extrapolations for  $\nu$

### 5.2.3 Corrections to the Gaussian variational approximation

Another approach that has been relatively successful in dealing with problems with self-avoidance is the Gaussian variational approximation [15]. It consists in approximating the exact density functional by the best possible quadratic weight for the field  $\vec{h}$ . It amounts to assuming that the self-avoiding term is not renormalized, that is  $Z_b = 1$ . The quantity  $\delta$  and the gyration radius exponent within this approximation were first computed in [3] with result

$$\begin{aligned}\delta_V &= \frac{-4\epsilon}{(D-1)(d+3)} \\ \nu_{var} &= \frac{7(D-1)}{(3d-5)}.\end{aligned}\tag{88}$$

The value for the physical tubule is  $\nu_{var} = \frac{7}{4}$ . This is clearly unphysical, being larger than one, but the accuracy of the Gaussian variational approximation should improve for large  $d$ , since it is essentially a large- $d$  expansion. As with the Flory approximation, we may determine the corrections to the Gaussian variational approximation within the  $\epsilon$ -expansion. From

$$\delta = \delta_V - \frac{4}{(D-1)(d+3)} \mu \frac{d}{d\mu} \log(Z_b),\tag{89}$$



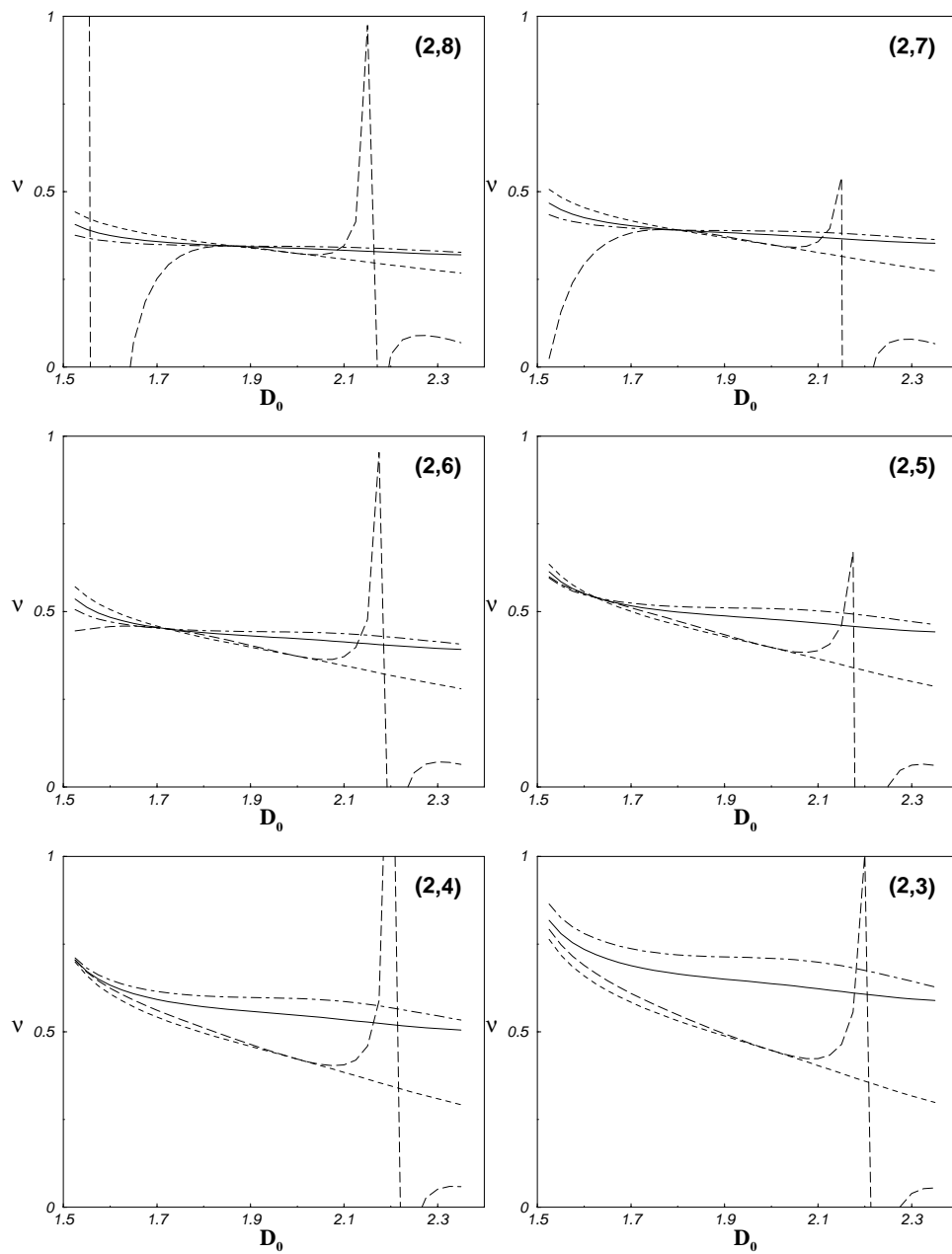


Figure 9: Corrections to the Flory estimate for  $\nu$ .

which consistently at lowest order in  $\varepsilon$  results in

$$\nu_V(D) = \frac{5 - 2D}{4} + \frac{\nu_1(D)}{D - 1}\varepsilon, \quad (90)$$

where  $\nu_1(D)$  is defined in Eq. 82 and again the extra factor appearing on the r.h.s is just 1 at  $D = 2$ , so Eq. 82 and Eq. 90 are equal at  $D = 2$ , as reported in [6].

Our extrapolations are summarized in Fig. 10. The Gaussian variational approximation turns out to be the least accurate of our determinations. At (2, 8) all different extrapolations deliver equivalent results, but the expansion C shows the flattest plateau. The situation is the same for the cases (2, 7), (2, 6) and (2, 5), but at (2, 4) and (2, 3), there are sizeable variations and there is no a clear plateau. For the sake of completeness, we extrapolate our results from this pseudo-plateau where variations are small, and quote an error bar from its variations, which are the results quoted in Table 2.

## 6 Conclusions

In this paper our first task was to identify the simplest free energy containing all the relevant operators controlling the large-distance physics of the tubular phase of anisotropic membranes. In this analysis essential use was made of rotational symmetries. Although our analysis may be modified by the existence of more complicated phase diagrams with non-perturbative fixed points in the spirit of [5], we believe that the model treated here reveals essential features of the physics of the anisotropic tubular phase.

Finally we completely characterized the phase diagram and calculated the critical exponents by generalizing the  $\varepsilon$ -expansion introduced in [6]. For the physical self-avoiding tubule we find

$$\nu = 0.62 \quad (91)$$

$$\zeta = 0.80 \quad (92)$$

$$z = 0.75 \quad (93)$$

$$\zeta_u = -0.33 \quad (94)$$

$$\eta_u = 1.65 \quad (95)$$

$$\eta_{\perp} = 1.0 \quad (96)$$

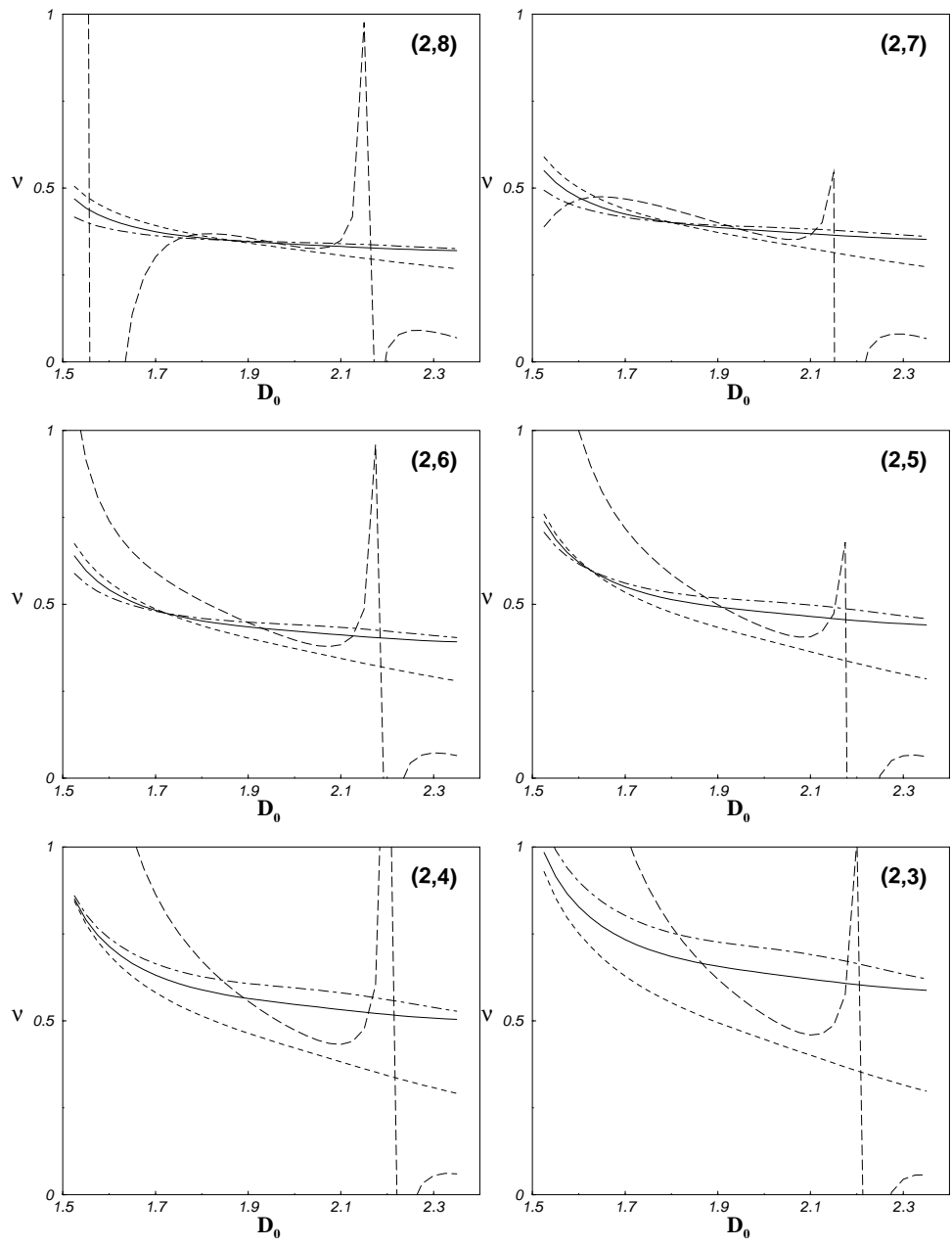


Figure 10: Corrections to the variational estimate for  $\nu$ .

Further improvement would necessitate a two-loop calculation for arbitrary  $D$  and would provide a valuable check of our extrapolation.

These predictions may be tested via an extension of the numerical simulations described in [7] to the much more demanding model with self-avoidance. These simulations are currently in progress. We hope the concreteness of the calculations presented here will inspire further work in the rich field of the physics of anisotropic extended manifolds.

## ACKNOWLEDGEMENTS

We thank Emmanuel Guitter, Leo Radzihovsky and John Toner for several valuable discussions on the subject matter of this paper. The research of M.B and A.T was supported by the U.S. Department of Energy under Contract No. DE-FG02-85ER40237.

## A Appendix

In this appendix we discuss the analytical properties of several functions that arise in the evaluation of the quantity  $I(D)$ . We follow closely the methods of [6], and rewrite Eq. 73 as

$$I(D) = \frac{1}{\Gamma(\frac{4D-3}{5-2D})} \int_0^{+\infty} dz F(z)^2 , \quad (97)$$

with

$$F(z) = z^{\frac{3D-4}{5-2D}} \int_0^{\infty} du u^{2D-3} e^{-zf(u)} , \quad (98)$$

and

$$\begin{aligned} f(u) = & u^{4-2D} \left\{ u \int_0^{+\infty} dt t^{\frac{D}{2}-1} K_{\frac{1-D}{2}}(t) \cos\left(\frac{t^{1/2}}{u}\right) \right. \\ & \left. + \frac{1}{2} \int_0^{+\infty} dt t^{\frac{D-3}{2}} K_{\frac{3-D}{2}}(t) \sin\left(\frac{t^{1/2}}{u}\right) \right\} , \quad (99) \end{aligned}$$

where  $K_\nu$  is a modified Bessel function. We have not been able to compute the integrals in Eq. 99 explicitly, except in the case  $D = 2$ . Nevertheless,

we know both that  $f(u)$  is a monotonically increasing function of  $u$  and its asymptotic behavior for small and large  $u$ . For large  $u$  we have the result,

$$f(u)_{u \rightarrow \infty} = 2^{\frac{D}{2}-2} \Gamma\left(\frac{1}{4}\right) \Gamma\left(\frac{D}{2} - \frac{1}{4}\right) u^{5-2D} (1 + \mathcal{O}(1/u)) \quad (100)$$

while, for small  $u$ , we have

$$\begin{aligned} \lim_{u \rightarrow 0} f(u) &= \frac{\pi \Gamma\left(\frac{3-D}{2}\right)}{2^{\frac{D+1}{2}}} \frac{1}{\Gamma(5-2D) \sin\left(\frac{\pi}{2}(5-2D)\right)} \\ \lim_{u \rightarrow 0} f^{(n)}(u) &= 0, \quad n > 0 \end{aligned} \quad (101)$$

where  $n$  stands for any derivative of  $u$ . The latter leads us to conjecture that the corrections to Eq. 101 are of the type  $\mathcal{O}(e^{-\frac{1}{4u^2}})$ , as explicitly seen at  $D = 2$ . A plot of  $f(u)$  for different values of  $D$  is given in Fig. 11.

The next step is to compute  $F(z)$  Eq. 98. Its exact analytical form seems hopeless to compute, but again we can find its asymptotic limits. For small  $z$  we have

$$F(z)_{z \rightarrow 0} = \frac{\Gamma\left(\frac{2D-2}{5-2D}\right)}{(2^{D/2-2} \Gamma(1/4) \Gamma(D/2 - 1/4))^{\frac{2D-2}{5-2D}} 5-2D} z^{\frac{D-2}{5-2D}} (1 + \mathcal{O}(z^{1/(5-2D)})), \quad (102)$$

and for large  $z$

$$F(z) \sim e^{-f(0)z}, \quad (103)$$

where  $f(0)$  is given by Eq. 101.

D	I(D)	D	I(D)
1.6	0.07951	2.0	1.263910 <sup>-3</sup>
1.7	0.04643	2.1	1.077510 <sup>-4</sup>
1.8	0.02027	2.2	1.7155710 <sup>-6</sup>
1.9	0.006434	2.3	4.0129810 <sup>-10</sup>

Table 3: Sample of values for  $I(D)$ .

The asymptotics provide valuable cross checks for the numerical integrations, and we have also used them in speeding up the numerical integration algorithms. A sample of values for  $I(D)$  is provided in Table 3.

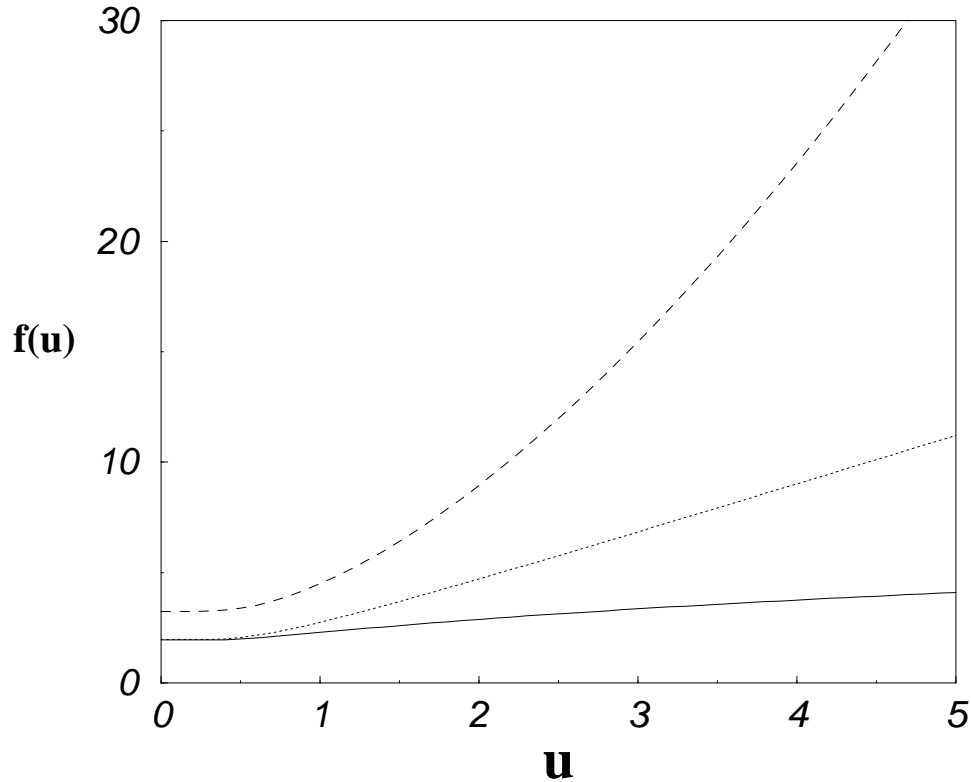


Figure 11:  $f(u)$  for different values of  $D$ . The dashed line is  $D = 1.7$ , the dotted line  $D = 2.0$  and the solid line  $D = 2.3$ .

## References

- [1] *Proceedings of the Fifth Jerusalem Winter School for Theoretical Physics*, edited by D. R. Nelson, T. Piran, and S. Weinberg (World Scientific, Singapore, 1989).
- [2] *Fluctuating Geometries in Statistical mechanics and Field Theory*, edited by F. David, P. Ginsparg and J. Zinn-Justin, Les Houches Session Vol. LXII (Elsevier, Amsterdam, 1996).
- [3] L. Radzihovsky and J. Toner, Phys. Rev. Lett. **75**, 4772 (1995).
- [4] D. Bensimon, private communication.

- [5] L. Radzihovsky and J. Toner, Phys. Rev. E **57**, 1832 (1998).
- [6] M. Bowick and E. Guitter, Phys. Rev. E **56**, 7023 (1997).
- [7] M. Bowick, M. Falcioni and G. Thorleifsson, Phys. Rev. Lett. **79**, 885 (1997).
- [8] K. Wilson and J. Kogut, Phys. Rep. **12C**, 75 (1974).
- [9] F. David, E. Guitter, S. Leibler and L. Peliti, Phys. Rev. Lett. **61**, 2949 (1988).
- [10] D. Amit, *Field Theory, the Renormalization Group, and Critical Phenomena*, World Scientific, Singapore (1984).
- [11] B. Duplantier, T. Hwa and M. Kardar, Phys. Rev. Lett. **64**, 2022 (1990).
- [12] F. David, B. Duplantier and E. Guitter, Phys. Rev. Lett. **70**, 2205 (1993); Nucl. Phys. B **394**, 555 (1993); Saclay Preprint T/97-001 *cond-mat/9702136*.
- [13] T. Hwa, Phys. Rev. A **41**, 1751 (1990).
- [14] F. David and K. Wiese, Phys. Rev. Lett. **76**, 4564 (1996); Nucl. Phys. B **487**, 529 (1997).
- [15] M. Goulian, J. Phys. II, 1327 (1991); P. Le Doussal, J. Phys. A **25**, L469 (1992).